



HAL
open science

A method to assess the impact of soil available water capacity uncertainty on crop models with a tipping-bucket approach

Julie Constantin, Victor Picheny, Lina Hadj Nassar, Jacques-Eric Bergez

► To cite this version:

Julie Constantin, Victor Picheny, Lina Hadj Nassar, Jacques-Eric Bergez. A method to assess the impact of soil available water capacity uncertainty on crop models with a tipping-bucket approach. European Journal of Soil Science, 2019, 71 (3), pp.369-381. 10.1111/ejss.12878 . hal-02618849

HAL Id: hal-02618849

<https://hal.inrae.fr/hal-02618849>

Submitted on 29 Aug 2023

HAL is a multi-disciplinary open access archive for the deposit and dissemination of scientific research documents, whether they are published or not. The documents may come from teaching and research institutions in France or abroad, or from public or private research centers.

L'archive ouverte pluridisciplinaire **HAL**, est destinée au dépôt et à la diffusion de documents scientifiques de niveau recherche, publiés ou non, émanant des établissements d'enseignement et de recherche français ou étrangers, des laboratoires publics ou privés.

The logo for the European Journal of Soil Science features the journal's name in white text on a dark brown, textured background that resembles soil. The words "European Journal of" are in a smaller font, while "Soil Science" is in a larger, bold font.

European Journal of **Soil Science**

A method to assess the impact of soil available water capacity uncertainty on crop models with tipping-bucket approach

Journal:	<i>European Journal of Soil Science</i>
Manuscript ID	EJSS-428-17.R4
Manuscript Type:	Original Manuscript
Date Submitted by the Author:	n/a
Complete List of Authors:	Constantin, Julie; AGIR, Université de Toulouse, INPT, INP-PURPAN, INRA Picheny, Victor; INRA MIA Hadj Nassar, Lina; INRA MIA Bergez, Jacques-Éric; AGIR, Université de Toulouse, INPT, INP-PURPAN, INRA
Keywords:	sampling, kriging, uncertainty quantification, drainage, yield

1 **A method to assess the impact of soil available water capacity**
2 **uncertainty on crop models with tipping-bucket approach**

3 J. CONSTANTIN^{a,*}, V. PICHENY^b, L HADJ NASSAR^b, J.-E. BERGEZ^a

4 ^a *AGIR, Université de Toulouse, INPT, INP-PURPAN, INRA, 31320, Castanet Tolosan,*
5 *France*

6 ^b *MIAT, Université de Toulouse, INRA, 31320, Castanet Tolosan, France*

7 * **Corresponding Author:** Julie Constantin (E-mail:julie.constantin@inra.fr).

8 **Running title:** *Critical Uncertainty of AWC in Crop Models*

9 **Summary**

10 Most agronomic crop models use a reservoir tipping-bucket approach to model the water
11 budget in the soil. Soil available water capacity (AWC) is the main soil property
12 considered in this approach. Because AWC is difficult to measure, uncertainty in AWC
13 may be high. We developed a method using a specific kriging technique to determine the
14 effects of uncertainty in AWC on crop model predictions. The AqYield crop model was
15 used as an example to assess the effects of uncertainty in AWC on two agronomic output
16 variables (grain yield and drainage). The factors considered were the climatic region, crop
17 type and soil depth. We assessed the results using the coefficient of variation (CV) and
18 sets of critical values for which CV exceeded 5%, 10% and 15%. The experiment
19 provided insight into the criticality of AWC uncertainty over a wide range of
20 agropedoclimatic situations according to crop, model and output of interest. The method
21 revealed the greater effect of AWC uncertainty on both outputs for the spring crop than
22 for the winter crop and to identify cases where AWC uncertainty was critical. There was
23 a stronger effect of AWC uncertainty on yield for shallow soil and climatic water deficit
24 conditions. For each situation, the AWC uncertainty levels were determined above or
25 below which the impact becomes significant on a given output since the sensitivity was
26 very dependent on climate-crop-soil combinations. It was also observed that uncertainty
27 in AWC had little effect in AqYield for a wide range of situations. The method developed
28 uses a small number of model simulations to produce accurate results to better understand
29 the impact of this major soil input data according to the target model and specific
30 objectives. It could help to determine the level of accuracy needed in AWC measurement
31 depending on the objectives.

32 **Keywords:** sampling, kriging, uncertainty quantification, drainage, yield

33 Highlights

- 34 • The method quantifies the effects of AWC uncertainty on crop models with a
35 tipping-bucket approach.
- 36 • This method can assess the impact of uncertainty with only a few runs using a
37 kriging approach.
- 38 • The method identifies critical situations for a wide range of agropedoclimatic
39 conditions.
- 40 • Critical region graphs give critical thresholds for accuracy needed in AWC.
- 41

42 **Introduction**

43 Many studies use modelling and simulation to analyze the effect of climate on agricultural
44 production or to determine the most suitable irrigation management practices (e.g.
45 Teegavarapu, 2010; Nendel et al., 2014; Ma et al., 2017). Most are based on the
46 description of a biophysical system that includes a crop and a soil component and daily
47 carbon, water and nitrogen fluxes in the soil-plant-atmosphere system influenced by
48 climate and cropping practices. Crop growth and development in such crop models are
49 simulated for a homogeneously managed plot at the one-dimension scale. Effects of
50 climate, soil properties, crop management and ecophysiological crop characteristics are
51 analyzed for different crops and environmental outputs (e.g. phenology, biomass
52 accumulation, grain yield, evapotranspiration, drainage, nitrate leaching, soil carbon
53 storage). Most agronomic crop models use a tipping-bucket approach to model the water
54 budget in the soil (Ritchie, 1981; Ranatunga et al., 2008). In this approach, the soil is
55 considered as a reservoir that provides a given amount of water. Precipitation and
56 irrigation (minus runoff) fill the reservoir, and losses are due to evapotranspiration and,
57 when the reservoir is full (i.e. at field capacity), drainage. Several representations, with
58 differing degrees of abstraction, exist, mainly dividing the soil into different layers subject
59 to different biological and physical processes (e.g. evaporation, transpiration, water
60 uptake, drainage). Available water capacity (AWC) is the main water-related property in
61 these layers.

62

63 Available water capacity is the maximum amount of water the soil can store that is
64 available for plant growth. It is an integrative value, determined throughout the entire soil
65 profile, from water content at field capacity to water content at the permanent wilting
66 point, below which a plant is unable to recover the remaining water (Behrman *et al.*,

2015). These two water content limits, whose physical definition remains under discussion (Czyz and Dexter, 2012), are empirical concepts and can have different meanings for soil scientists, agronomists and ecophysicologists. However, AWC is a widespread concept used in many crop models. Different approaches are used to estimate AWC: (i) measurements (e.g. field experiments with different crops to analyze effects of several irrigation regimes by proxy sensor measurements, in-situ water content monitoring, and laboratory measurements of soil cores in pressure chambers) (e.g. Veihmeyer and Hendrikson, 1949); (ii) pedotransfer functions, which are statistical relationships (e.g. with texture, bulk density and organic matter) that are more easily determined (e.g. Bruand et al., 2004); and (iii) optimization processes that use inverse modeling of crop models to compare model outputs and real observations of the soil-plant-atmosphere system, such as soil moisture, crop leaf area index or evapotranspiration (e.g. Guerif et al., 2006).

80

Whether measured or statistically estimated, uncertainty in the AWC may be considerable, which might influence the quality of crop model predictions. Sensitivity analyses of crop models have demonstrated the sometimes strong but not systematic influence of uncertainty in AWC or its components (e.g. field capacity or wilting point) on predictions of yield, soil water content or annual drainage for instance (Aggarwal, 1995; Lawless *et al.*, 2008; Varella *et al.*, 2012). The uncertainty here is as defined by Spiegelhalter and Riesch (2011) as the uncertainty essentially due to limitations in information, in particular, a lack of quality or accurate data. It concerns input data uncertainty, which is one of the three main sources of uncertainty in modelling, along with parameter data and model structure (Walker et al., 2003). Information about AWC may be limited for several reasons. In soil considered as homogeneous, there is still some

92 spatial variability in its properties, and there are some uncertainties in the methods used
93 to measure AWC directly. In the case of pedotransfer functions, applied to a national
94 database, for instance, there is uncertainty in soil parameters such as clay content, soil
95 depth and soil organic matter, as well as on the function chosen that uses this information
96 to estimate field capacity and permanent wilting points. Usually, the distribution for these
97 parameters is unknown, and the uncertainty can be large.

98

99 Consequently, the main research question is: “How important is accuracy in estimating
100 the AWC and to what extent does the level of accuracy depend on soil properties, climate
101 and crop species?” Depending on the weather, crop and management practices, the
102 accuracy in AWC may influence the accuracy of simulation model predictions. The
103 objective of our study was to develop a modelling approach to quantify the effects of
104 uncertainty in AWC on agronomic model predictions according to the crop type, climate
105 and soil depth and to identify critical thresholds for accuracy. This differs from a classic
106 sensitivity analysis, since we aim to define critical sets of input variables that provide a
107 given accuracy in output variables.

108

109 **Materials and Methods**

110 *AqYield crop model overview*

111 AqYield is a simple and generic crop model that simulates crop production and water
112 balance at a daily time-step (Fig. 1). A complete description of the model and its quality
113 of prediction for different crops and soil and climate conditions can be found in
114 Constantin et al. (2015). The model was designed to be generic, i.e. simulating several
115 crops using one single approach and changing only crop parameters. Crop phenology is

116 defined by three stages as a function of thermal time corrected with photoperiodic effects
117 for winter crops: emergence, flowering and physiological maturity. Crop development is
118 simulated using a crop coefficient to calculate water requirements, and root elongation is
119 used to estimate the available water in the soil. The model does not simulate biomass
120 growth; it calculates yield at harvest using a production function based on the water stress
121 during the crop development period and a maximum yield that is an input of the model.
122 Soil is simulated using a tipping-bucket approach. The user inputs clay content, depth and
123 AWC throughout the entire soil profile. Available water capacity in the model is the
124 maximal water content available for the crop over the soil depth reachable by roots. It is
125 usually defined as the water amount between the wilting point and field capacity. AqYield
126 simulates water-balance components (e.g. evaporation, transpiration, drainage and
127 runoff) and the daily soil water content above wilting point. AqYield is simpler than other
128 crop models (Palosuo *et al.*, 2011; Rötter *et al.*, 2012) and is well suited to demonstrate
129 our approach. It is important to highlight that AqYield was chosen to illustrate the method
130 we developed, not to understand the model's internal behaviour better.

131 *Figure 1*

132 *Identifying thresholds*

133 *AWC uncertainty and probability distribution law*

134 In our approach, AWC was considered as an uncertain input in the AqYield model. A
135 classic approach is to perform simulation-based uncertainty propagation. More formally,
136 given X , a random input variable with known distribution $\mathcal{F}(X)$, the output of interest
137 $Y=f(X)$ with f the AqYield model is also random, with (unknown) distribution $\mathcal{F}(Y)$. To
138 quantify the uncertainty in the output variable (Y), we used the coefficient of variation
139 (CV), according to Varella *et al.* (2012). The CV of output Y was defined as $CV(Y) = \frac{\sigma(Y)}{E(Y)}$,

140 with σ the standard deviation and E the mathematical expectation. $CV(Y)$ can be
 141 considered a function of the input distribution $\mathcal{F}(X)$. Our objective was to find at what
 142 values of $\mathcal{F}(X)$ $CV(Y)$ reached a critical level (a maximum variation in the output chosen
 143 by the model user depending on the user's objectives). Here, we chose grain yield (t ha⁻¹)
 144 and water drainage (mm).

145

146 Without losing generality in the approach, we assumed that AWC followed a uniform
 147 distribution (\mathcal{U}) between a lower (X_L) and upper boundary (X_U), $\mathcal{F}(X)=\mathcal{U}(X_L,X_U)$, which
 148 we characterized by its mean and standard deviation ($\mu_X = \frac{X_L + X_U}{2}$ and $\sigma_X = \frac{X_U - X_L}{\sqrt{12}}$,
 149 respectively). Next, we defined the set of critical values $\mathcal{F}(X)$ as all pairs (μ_X, σ_X) for
 150 which the CV exceeded a given threshold: $\Omega_c = \{(\mu_X, \sigma_X) \text{ such that } CV(\mu_X, \sigma_X) > \alpha\}$. We
 151 chose three values for α : 5%, 10% and 15%, which are common levels of CV for
 152 experimental results in agronomy (Bassu et al., 2014). Our objective was then to identify
 153 the critical region(s) Ω_c in the (μ_X, σ_X) plane.

154

155 Since the AqYield model is considered as a (non-linear) "black-box", the distribution
 156 $\mathcal{F}(Y)$ can be inferred (using parametric or non-parametric techniques) only by drawing
 157 random samples of X for a given pair (μ_X, σ_X) , $\{X_1, \dots, X_n\}$ and evaluating model outputs
 158 for these samples: $\{Y_1 = f(X_1), \dots, Y_n = f(X_n)\}$. For CV , one may simply use the empirical

159 estimator $\widehat{CV}(Y) = \frac{\sigma(Y_1, \dots, Y_n)}{E(Y_1, \dots, Y_n)}$.

160

161 Obtaining accurate estimates requires a sufficient sample size n ; however, sample size is
162 limited by computational resources because it directly determines the number of runs of
163 AqYield.

164 *Kriging*

165 A typical way to obtain the set Ω_c is to discretize the $\{\mu_X, \sigma_X\}$ domain across a grid and
166 calculate $\widehat{CV}(Y)$ for all value combinations. However, this approach would result in
167 overly-intensive simulation experiments because even a coarse grid (10 μ_X values \times 10 σ_X
168 values) with $n=100$ replicates would require 10,000 runs of AqYield. Instead, we
169 followed the strategy developed by Picheny et al. (2010) that relies on the kriging model,
170 as follows:

- 171 1. CV is calculated for an initial set of nine pairs of (μ_X, σ_X) evenly distributed in the $(\mu_X,$
172 $\sigma_X)$ space.
- 173 2. A kriging model is fitted to these data.
- 174 3. Nine additional pairs of (μ_X, σ_X) for which CV is calculated are chosen sequentially
175 according to a criterion calculated using the kriging model (namely the *targeted IMSE*
176 *criterion* of Picheny et al. (2010)), the model being updated after each new CV value
177 is calculated.

178 In brief, after the initialization step, the kriging-based approach iteratively chooses new
179 observations so that the boundary between critical and non-critical regions (i.e. where the
180 CV exceeds or does not exceed the threshold, respectively) quickly becomes accurate.
181 The numbers of initial and additional pairs required to obtain an accurate kriging model
182 generally depends on the problem. We determined that nine initial observations followed
183 by nine sequential observations provided a reasonable trade-off between kriging accuracy

184 and computational cost. This number is in line with the classic kriging rule-of-thumb of
185 setting the number of observations equal to 5-10 times the dimension (here, two).

186

187 The sequential strategy was conducted using the R package KrigInv (see Chevalier et al.,
188 2014 for more details about its theoretical elements and implementation). The kriging
189 equations and relevant technical details are provided in the Supporting Information, along
190 with an illustration of the method.

191 *Experimental design*

192 We analyzed two crop model outputs to evaluate effects of uncertainty in AWC: (i) yield,
193 for the influence on crop production, and (ii) cumulative water drainage during crop
194 development, for the influence on an environmental variable (Table 1). We selected two
195 major crops: winter wheat (winter crop) and sunflower (spring rainfed crop). Winter
196 wheat was simulated from 1 October to 10 July and sunflower from 1 May to 1 October,
197 both starting with maximum AWC at sowing. Both crops were assumed to be limited only
198 by water (well fertilized and well protected against pests and diseases). Crop variety
199 remained the same for each crop regardless of the soil, site or climate. Sunflower reached
200 physiological maturity at 1720°C-days (base 4.8°C) and wheat at 2015°C-days (base
201 0°C). For both sites, based on statistics from both regions
202 (<https://stats.agriculture.gouv.fr/disar-web/accueil.disar>), maximum yield was defined as
203 7.3 and 4.2 t ha⁻¹ for winter wheat and for sunflower, respectively, using the highest values
204 found in the statistical data since it is a potential yield.

205

Table 1

206 To test our method, two 15% clay soils were selected: a 0.8 m shallow soil and a 1.5 m
207 deep soil. We chose soils with contrasting depth, hypothesizing that a user would have

208 some prior knowledge about the soil and that the impact of AWC uncertainty may vary
209 with the amount of total available water in the soil and its availability for the crop during
210 its development. For each soil, we assumed that the volumetric AWC ranged from 0.10-
211 0.16 $\text{mm}_{\text{water}} \text{mm}_{\text{soil}}^{-1}$. This range was chosen from field experiment measurements
212 obtained during the RUEdesSOLS project (unpublished data). Multiplying soil depth by
213 the volumetric AWC yielded AWCs of 80-140 mm for the shallow soil and 140-240 mm
214 for the deep soil. As a result, μ_X varied from 80-140 mm and σ_X from 0-50 mm for shallow
215 soil. For deep soil, μ_X varied from 140-240 mm and σ_X from 0-50 mm.

216 We chose two contrasting sites for climate data, one in southwestern France (Toulouse,
217 43° 33' N, 1° 26' E) and one in western France (Poitiers, 46° 33' N, 0° 17' E), in regions
218 where both crops are cultivated. Our initial climate data consisted of daily measurements
219 of mean temperature, potential evapotranspiration (PET) and precipitation from 1975-
220 2012. Because the effect of uncertainty in AWC may depend greatly on weather
221 conditions, due to the large difference in water inputs that can occur, we performed the
222 analysis using a representative set of climates. To simplify the approach (see next
223 section), we classified the 38 years of records into four types of climates for each site
224 (Warm&Dry, Warm&Wet, Cold&Dry, Cold&Wet). For each crop development period,
225 we first calculated the thermal time (TT, in °C-days) to split the dataset into warm and
226 cold years for each crop according to its base temperature (0°C and 4.8°C for wheat and
227 sunflower, respectively). Then, each subset was split in half again according to a water
228 deficit indicator (WD_c , in mm), and calculated as the cumulative difference between
229 precipitation and PET, to distinguish dry and wet years. The division was based on
230 median values to obtain four subsets of equal size. Finally, the year closest to the centre
231 of each subset (Euclidian distance) was selected as that subset's representative year.

232 *Modelling and simulation*

233 AqYield was used in the modelling and simulation platform RECORD (Bergez et al.,
234 2013), which creates and connects models with a graphical user interface (using a “box
235 and arrow” approach) and performs multiple simulations. All simulations were performed
236 using R (R Core Team, 2014) and the “rvle” package ([http://www.vle-project.org/vle-](http://www.vle-project.org/vle-11/rvle/)
237 [11/rvle/](http://www.vle-project.org/vle-11/rvle/)) to run models in RECORD directly under R. Our experiments required 115,200
238 runs of AqYield to generate for one output all the graphs for the 32 conditions (2 sites ×
239 4 climate types × 2 soil depths × 2 crops); the model also required 3600 runs for the three
240 α levels.

241

242 **Results**

243 *Presenting kriging results in “critical region” maps*

244 Using the kriging approach, we are able to represent, for a given soil depth, climate region
245 and crop type, a threshold value and intervals of variation for both AWC mean and
246 standard deviation, the corresponding map of the critical region in the (μ_X, σ_X) space.
247 Since the critical region corresponding to a given threshold is a subset of the region
248 corresponding to a smaller threshold, we represent the three critical regions (for $\alpha= 5\%$,
249 10% and 15%) in a single graph (Fig. 2). With this approach, unfavourable combinations
250 of AWC mean and standard deviation as a function of the targeted level of uncertainty
251 can be directly identified.

252

Figure 2

253 In the example (Fig. 2), CV exceeds 15% at small μ_X values and large σ_X values.
254 Conversely, at large μ_X values, even high uncertainty has little effect on the output; for

255 example, an AWC of 125 ± 50 mm leads to a stable prediction of yield (variation below
256 15%). If the acceptable variability is smaller, 10% for instance, for an expected value of
257 125 mm AWC, the uncertainty should not exceed ± 35 mm.

258

259 In addition to the graphical representation, we calculated the average critical region as a
260 summary measure (Fig. 2, approximately 0.18 for $\alpha=15\%$). In this example, this critical
261 region of 0.18 means that 18% of the set of distributions considered for AWC (the $(\mu_X,$
262 $\sigma_X)$ space) leads to variability in yield prediction above the chosen threshold.

263 *Climate selection*

264 As expected, the climate in Toulouse was warmer and drier than that in Poitiers during
265 the periods of sunflower and wheat crop development (Fig. 3). During sunflower
266 development, WD_c ranged from -572 mm to -238 mm in Toulouse and -388 to -167 mm
267 in Poitiers, while TT ranged from 2010-2336°C-days in Toulouse and 1752-1999°C-days
268 in Poitiers. During winter wheat development, WD_c ranged from -249 to +114 mm in
269 Toulouse and +7 to +271 mm in Poitiers, while TT ranged from 2599-3011°C-days in
270 Toulouse and 2282-2643°C-days in Poitiers.

271 *Figure 3*

272 Regardless of the crop, the same type of climate always had higher TT and lower WD_c in
273 Toulouse than in Poitiers (Table 2). As expected, the spring crop had a greater WD_c than
274 the winter crop. Dry years were drier in hot years than in cold years, and wet years were
275 wetter in cold years than in hot years.

276 *Table 2*

277 *Agronomic results*

278 The model slightly overestimated grain yield compared to those in regional statistics,
279 which is not surprising since AqYield cannot represent all limiting factors. As expected,
280 yield was lower, by 0.71 and 0.58 $t_{DM} ha^{-1}$ on average for sunflower and wheat,
281 respectively, and drainage was slightly higher, by 8 and 4 mm on average under sunflower
282 and wheat, respectively, in shallow soils than in deep soils regardless of the climate, site
283 and crop (Fig. 4). No general trend was observed regarding the site, but yields tended to
284 be lower when the climate was drier, because of greater water stress due to greater WD_c .
285 On average, the water stress index was 0.50 and 0.64 (1 = no stress) in dry years and 0.67
286 and 0.73 in wet years for sunflower and wheat, respectively. The standard deviation of
287 yield was always higher for shallow soils than for deep soils due to the greater variation
288 in yields from 30 to 190 mm AWC, which implies different levels of water stress (from
289 0.42 to 0.73, respectively, on average). Yields were much more stable in deep soil, where
290 the AWC ranged from 90-290 mm, due to the absence of impact of AWC on water stress,
291 which remained stable on average.

292

293 The amount of drainage depended greatly on the length and timing of crop development
294 with, on average, 42 mm under sunflower compared to 265 mm under wheat. Since
295 sunflower grew for five months in spring and summer, precipitation and then drainage
296 during its development were lower than those during winter wheat development, which
297 lasted nine months and included winter precipitation. In fact, mean precipitation was 277
298 mm under sunflower vs. 539 mm under wheat. Significant site effects were predicted for
299 drainage under wheat, which was twice as high in Poitiers (353 mm) as in Toulouse (176
300 mm).

301

Figure 4

302 *Effects of uncertainty in AWC on yield and drainage*

303 We present here the main results in the form of an average critical region (Table 3) and
304 probability of critical region (Fig. 5) for the 32 agropedoclimates. The critical region of
305 the thresholds always followed this order: 5% threshold \geq 10% threshold \geq 15% threshold
306 (Table 3). This was due simply to the smaller degree of tolerance for variation in output
307 at 5% than at 15%.

308 *Table 3*

309 The effect of uncertainty in AWC ranged from never critical (area=0.00) to highly critical
310 (area=0.99), with many intermediate situations. Unexpectedly, for approximately two-
311 thirds of the simulated cases, AWC uncertainty was not critical for either model output.
312 Uncertainty in AWC had greater effects on the two outputs when simulating sunflower
313 (spring crop) than when simulating winter wheat (winter crop), which could be due to
314 different crop sensitivity to water stress. For example, the critical region at the 15%
315 threshold reached a maximum of 0.81 for sunflower yield but was always 0.00 for wheat
316 yield (i.e. for the set of distributions considered for AWC, 81% and 0% led to excessive
317 variability in yield prediction for sunflower and wheat, respectively). The crop also had
318 a strong influence on drainage, with one-third of cases having 0.35 critical region at the
319 10% threshold for sunflower, while no case exceeded 0.01 critical region for wheat. In
320 some cases for sunflower, the critical region reached 0.99, meaning that even a small
321 uncertainty had a large impact on drainage. Conversely, the critical region for wheat was
322 almost always 0.00 for yield and drainage at 10% and 15% thresholds.

323

324 The critical region for yields was higher for shallow soil than for deep soil. For sunflower,
325 the critical region at the 5% threshold ranged from 0.00-0.20 for deep soil and from 0.13-
326 0.95 for shallow soil. It was lower at the 15% threshold but still reached 0.81 in the

327 Hot&Dry climate. Certain situations remained sensitive to uncertainty in AWC when the
328 threshold was changed to 15%, such as the Hot&Dry climate in Poitiers in shallow soil,
329 which had a critical region of 0.81. The critical regions for wheat yield were lower than
330 those for sunflower, with 0.00-0.01 for deep soil and 0.00-0.44 for shallow soil at the 5%
331 threshold. Areas tended to be larger in a Hot&Dry climate than in a Wet&Cold climate
332 for both crops on yield.

333 For drainage, the influence of climate was less clear, especially for sunflower. The period
334 of crop development (spring vs. winter) seemed to be the main factor. Drainage under
335 sunflower was more sensitive to uncertainty in AWC than that under wheat, for which
336 uncertainty in AWC had no influence except for two cases in Toulouse. In Dry&Hot years
337 in Toulouse for both soil depths and in Poitiers for deep soil, drainage was null under
338 sunflower; so, uncertainty in AWC had no influence, regardless of its value. The
339 Hot&Dry climate in Toulouse had no critical region due to the lack of drainage. Soil depth
340 also influenced drainage sensitivity to uncertainty in AWC, with more sensitivity in
341 shallow soil than in deep soil. However, effects of uncertainty could be substantial in deep
342 soil, such in the Cold&Wet climate in Toulouse or the Hot&Wet climate in Poitiers,
343 which had critical regions greater than 0.45 at the 15% threshold. Fig. 5 shows all
344 simulation results and graphs of the critical regions reported in Table 3. The main
345 differences occurred in yield and drainage between sunflower and winter wheat, followed
346 by differences in sunflower yield between shallow and deep soils. Depending on the
347 graph, the critical region did not occur for the same AWC mean and standard deviation
348 combination and three main patterns can be distinguished.

349 *Figure 5*

350 In the first pattern, AWC mean and standard deviation do not influence the output of
351 interest greatly in a specific context (Fig. 5, dark grey only). In the second pattern, critical

352 AWC uncertainty occurred for small mean and large standard deviation (Fig. 5, top left
353 of graphs). The second pattern was found mostly on yield response to AWC but on some
354 drainage response as well (e.g. {Cold&Dry, Toulouse, Shallow soil, Winter wheat}). This
355 pattern allows, for each condition and threshold, two interesting values to be determined:
356 the mean AWC above which uncertainty has no impact on the output of interest and the
357 uncertainty below which the output does not vary more than the threshold, regardless of
358 the mean AWC. In the third pattern, critical AWC uncertainty occurred when both
359 standard deviation and mean AWC were large, as on drainage (Fig 5, top right of graphs)
360 (e.g. {Cold&Dry, Poitiers, Shallow soil, Sunflower}). This pattern also shows some
361 interesting thresholds, such as the mean AWC below which uncertainty matters little or
362 not at all. These graphs complement quantitative critical regions (Table 3) since they can
363 be used to define such thresholds and identify combinations of mean and standard
364 deviation of AWC for which uncertainty matters or does not.

365 **Discussion**

366 *The method developed*

367 Our experiments enabled the identification of critical situations of AWC uncertainty for
368 a given output and variation threshold (Fig. 4 & 5). Transferring this method to more
369 computationally demanding and sophisticated models potentially raises two challenges.
370 First, the maximum feasible number of runs may decrease greatly. Second, the shape of
371 critical AWC uncertainty areas might become more complex, which requires more model
372 runs to provide an estimate. Our approach accommodates such a framework because the
373 combined use of kriging models and adaptive sampling has been shown to be an efficient
374 alternative when data are scarce, even for multimodal functions (Picheny et al., 2010).
375 The number of runs required to estimate a single CV value (n , see section 2.2) can be

376 drastically reduced (e.g. to a dozen) as long as the kriging model accounts for the loss of
377 accuracy (Ankenman et al., 2009). A more complex but more efficient solution could be
378 to fit a single kriging model to all conditions by considering conditions as qualitative
379 factors (Qian et al., 2012).

380

381 The uniform distribution to model uncertainty in AWC was chosen since we did not have
382 information about the actual distribution. A different distribution (e.g. triangular,
383 truncated normal) can be used without changing our method; however, in a preliminary
384 study, we found that it had little influence on *CV* areas of exceedance (data not shown).

385 This method, applied to AWC in this study, can also be used to determine the degree of
386 accuracy needed for other input parameters in a particular context and for a given crop
387 model. It may be relevant to apply it to important input data that are uncertain, such as
388 soil properties, like AWC in this study.

389 *Data sampling and accuracy*

390 This method can determine several key values, such as the AWC value above which
391 uncertainty does not influence the output of interest above a chosen threshold. It can also
392 assess the uncertainty in AWC below which, regardless of the AWC, this uncertainty does
393 not influence the output above the threshold. These types of quantification are not easily
394 accessible information and likely depend on the model chosen, as well as the
395 agropedoclimatic conditions considered. If one has prior knowledge of the type of
396 climate, the crop and desired outputs, the method can determine the degree of accuracy
397 required to estimate soil AWC used as input for a specific model. Therefore, our method
398 could identify situations in which accuracy in AWC is not important and situations in
399 which it is essential for the chosen model. This could save time and resources to focus on

400 more important inputs under specific conditions. It could also help to choose the most
401 suitable methods to estimate or measure AWC, with differing degrees of accuracy
402 according to the research objective. For example, if uncertainty in AWC has little
403 influence on the model output of interest, one can choose a small number of soil
404 measurement replicates to sample. In contrast, it could be important to have as little
405 uncertainty as possible and increase the number of samples to obtain an accurate AWC.
406 Thus, the influence of uncertainty in AWC can be analyzed prior to measurements to
407 provide recommendations for measuring it.

408 *Effects of uncertainty in AWC for the AqYield model*

409 This analysis shows that, for yield, uncertainty in AWC influenced spring crop
410 predictions more than winter crop predictions due to less precipitation during sunflower
411 development and the absence of irrigation, especially in dry climates. We expected this
412 result according to previous knowledge on water availability and crop production (e.g.
413 Zhang & Oweis, 1999; Pandey *et al.*, 2000). Since potential yield was lower for sunflower
414 ($4.2 \text{ t}_{\text{DM}} \text{ ha}^{-1}$) than for wheat ($7.5 \text{ t}_{\text{DM}} \text{ ha}^{-1}$), a smaller absolute variation in sunflower yield
415 was required to exceed a given threshold. If the potential yield were higher than the ones
416 we chose here, larger absolute variation would have been required to reach the critical
417 thresholds and conversely if they were lower. In fact, using the CV induces higher
418 sensitivity to small mean values, which may not be relevant for all outputs.

419

420 Notably, our study highlights that the accuracy in AWC measurements or estimates is not
421 important in two-thirds of the cases in our simulation experiment, for both outputs. This
422 result is consistent with that of Vanuytrecht *et al.* (2014), indicating that model sensitivity
423 to parameter uncertainty depends on agropedoclimatic conditions. Like these authors, we

424 found that uncertainty in soil water properties has more influence on yield when
425 environmental conditions induce water stress. In deep soil, our analysis shows that ± 40
426 mm of uncertainty in AWC has no significant effects on simulated wheat yield regardless
427 of the climate or sunflower yield in several climates because it did not change the degree
428 of water stress significantly. Consistent with other studies on yield and AWC (Lawless *et*
429 *al.*, 2008), greater accuracy in AWC is needed for shallow soil due to the greater water
430 stress induced by low AWC. In our method, the minimum level of accuracy needed can
431 be determined using graphical analysis (Fig. 5). For instance, uncertainty in AWC
432 measurement less than ± 20 mm has no influence on winter wheat yield.

433

434 For drainage, unlike with yield, in several cases uncertainty in AWC had great influence
435 in both shallow and deep soils. Interestingly, for a given AWC, the critical level of
436 uncertainty changed with soil depth (e.g. for sunflower, at AWC = 140 mm, the critical
437 uncertainty was sometimes lower in shallow soil than in deep soil (Fig. 5)). In this case,
438 drainage was higher in the deep soil than in the shallow one, as opposed to the general
439 tendency presented in figure 4. This trend is due to a difference in evaporation from the
440 soil. Available water capacity of the layer where evaporation can occur is reduced in the
441 deep soil, with less water available at the surface. As a result, drainage is higher in deep
442 soil than in shallow soil for the same AWC. It takes a larger change in drainage due to
443 AWC uncertainty to reach the critical threshold since the coefficient of variation depends
444 on the mean value. Given the formula for calculating the coefficient of variation (division
445 by the average value), to reach the same percentage requires a larger change in absolute
446 value if the average value is higher.

447

448 The size of the critical region depended greatly on the crop, due mainly to the period of
449 development. Drainage under sunflower was low (usually < 100 mm), and small changes
450 in its value due to uncertainty in AWC caused it to cross the critical threshold, while
451 larger changes were required for winter wheat drainage. The choice of the threshold (here,
452 5%, 10% and 15%) should consider this fact in combination with the purpose of the study.
453 Comparing the two outputs reveals that they do not respond in the same way, and critical
454 cases in which accuracy in AWC is needed are not necessarily the same. This is due to
455 differences in mechanisms driving these outputs, which indicates that, for other outputs,
456 the method needs to be applied to determine their sensitivities to uncertainty in AWC.

457 *Application to other soils, climates and sites*

458 Two soils of contrasting depth were studied to show the potential interaction between
459 crop development, soil depth and AWC uncertainty. As hypothesized, soil depth can
460 change the critical conditions for AWC uncertainty and should be considered in future
461 studies if it is known. If not, the method can be applied to a continuum from low to high
462 AWC and even with increased uncertainty in AWC if relevant (e.g. for some soil types).
463 The study simulated four climate years at each of two contrasting sites, which represents
464 non-exhaustive diversity in climate; however, it does identify several trends according to
465 the type of climate. Based on our results for the two sites, we can extrapolate that in wetter
466 climates than those tested, uncertainty in AWC would have less influence on yield due to
467 less water stress and little or no influence on winter drainage due to the increase in
468 drainage with more precipitation. We also expect AWC to have less influence in summer
469 due to the increase in drainage, which then requires more absolute variation to exceed the
470 critical threshold.

471

472 In climates drier than those studied, summer drainage under sunflower, for instance,
473 would tend to be null, and uncertainty in AWC would no longer have an influence, while
474 winter drainage would decrease and probably become more sensitive to uncertainty in
475 AWC than that in dry years in Toulouse. For yield, a drier climate might have a stronger
476 influence with less AWC, especially spring crops. When irrigation is introduced, the
477 importance of uncertainty in AWC for yield predictions decreases greatly because more
478 water is available to the crop, becoming more similar to the results of the wet climate
479 simulated.

480

481 For a given site, selecting four contrasting years in a 38-year time series allowed us to
482 explore a good part of the climatic variability while limiting the number of simulations,
483 even though it did not represent the more extreme years. Since we classified and selected
484 the “representative” years for each crop according to important climatic variables
485 (temperature and precipitation minus potential evapotranspiration), we obtained good
486 representation of climate variability for spring and winter crops at these sites. Statistical
487 analysis of the 38 years of climate could be useful for extrapolating our results and
488 calculating the probability of AWC uncertainty having a high influence and the need for
489 accurate measurements. Nevertheless, if one is interested in extreme years, these years
490 should be analyzed using the method developed. As mentioned, while some extrapolation
491 is possible, it is interesting to apply this method to specific conditions to assess the pattern
492 of response to and useful threshold of AWC uncertainty.

493 *Use of other models*

494 The method we developed and applied to the AqYield model as an example is applicable
495 to other crop models. AqYield used AWC throughout the soil profile as a direct input, but

496 crop models using field capacity and wilting points as inputs to calculate AWC would
497 need to have consistent variations in these two soil parameters generated first. Since all
498 models do not necessarily have the same response to water stress and availability,
499 predictions and sensitivity to AWC uncertainty can differ. A trend similar to that observed
500 for AqYield would probably occur since crop models simulate the same phenomenon, but
501 with different degrees of uncertainty above which outputs would change significantly.
502 Another potential extension is to apply our method to other input parameters, such as soil
503 clay content, initial biomass of a perennial crop, and initial nitrogen or carbon content of
504 the soil.

505 *Consequences for water management*

506 We simulated crops without irrigation because rainfed systems are expected to be the
507 most sensitive to uncertainty in AWC. Regarding irrigation and the influence of
508 uncertainty in AWC on water management, uncertainty in AWC may have an influence
509 on beginning and ending dates for irrigation and also change the frequency and amount
510 of irrigation (Bergez et al., 2001). However, for uncertainty in AWC to have an influence
511 on irrigation, indicators used to trigger irrigation should be related to the AWC. Typical
512 indicators such as dates, precipitation and phenological stages are not directly related to
513 AWC; in contrast, tensiometer indicators, closely related to AWC, are most often used.
514 In the latter case, the influence of AWC uncertainty on irrigation management could be
515 quantified.

516

517 **Conclusion**

518 This study developed a method to identify critical thresholds for uncertainty in AWC,
519 according to specific conditions of climate, soil, crop and outputs of interest. It allows,

520 with a limited number of simulations, to assess the critical conditions for which a given
521 output is influenced by uncertainty in this major input variable in a crop model using a
522 tipping-bucket approach. In this case study, it has highlighted in which cases AWC has a
523 significant impact and identified the numerous situations where the outputs were not
524 sensitive to AWC uncertainty due to the climatic conditions. The method is not specific
525 to AWC and can be applied to other model parameters that are uncertain and assumed to
526 influence outputs of interest, such as AWC, that are major inputs, difficult to measure
527 accurately and that can influence crucial water resources. This method can be applied to
528 other models, with some adaptation of wilting point and field capacity input instead of
529 AWC, and conditions depending on the objectives of future studies. It can give some
530 indications to choose the effort needed to measure model input parameters as a function
531 of the influence of their uncertainty on the outputs of interest.

532

533 **Acknowledgments**

534 This study was funded by the ANR project RUEdesSOLS (ANR-14-CE01-0011).

535

536 **Data availability statement**

537 Data available on request from the authors

538

539 **References**

540 Aggarwal, P.K. 1995. Uncertainties in crop, soil and weather inputs used in growth
541 models: Implications for simulated outputs and their applications. *Agricultural Systems*,
542 48, 361–384.

- 543 Ankenman, B., Nelson, B.L. & Staum, J. 2009. Stochastic kriging for simulation
544 metamodeling. *Operations Research*, 58, 371-382.
- 545 Bassu, S., Brisson, N., Durand, J.-L., Boote, K.J., Lizaso, J., Jones, J.W., Rosenzweig,
546 C., Ruane, A.C., Adam, M., Baron, C., Basso, B., Biernath, C., Boogaard, H., Conijn,
547 S., Corbeels, M., Deryng, D., De Sanctis, G., Gayler, S., Grassini, P., Hatfield, J., Hoek,
548 S., Izaurrealde, C., Jongschaap, R., Kemanian, A.R., Kersebaum, K.C., Kim, S.-H.,
549 Kumar, N.S., Makowski, D., Müller, C., Nendel, C., Priesack, E., Pravia, M.V., Sau, F.,
550 Shcherbak, I., Tao, F., Teixeira, E., Timlin, D. & Waha, K. 2014. How do various maize
551 crop models vary in their responses to climate change factors? *Glob. Chang. Biol.* 20,
552 2301–20. doi:10.1111/gcb.12520
- 553 Behrman, K.D., Norfleet, M.L. & Williams, J. 2015. Methods to estimate plant
554 available water for simulation models. *Agric. Water Manag.* 175, 72–77.
555 doi:10.1016/j.agwat.2016.03.009
- 556 Bergez, J.-E., Chabrier, P., Gary, C., Jeuffroy, M.H., Makowski, D., Quesnel, G.,
557 Ramat, E., Raynal, H., Rouse, N., Wallach, D., Debaeke, P., Durand, P. Duru, M.
558 Dury, J., Faverdin, P., Gascuel-Oudou, C. & Garcia, F. 2013. An open platform to
559 build, evaluate and simulate integrated models of farming and agro-ecosystems.
560 *Environmental Modelling and Software*, 39, 39-43.
- 561 Bergez, J.-E., Debaeke, Ph., Deumier, J.-M., Lacroix, B., Leenhardt, D., Leroy, P. &
562 Wallach, D. 2001. MODERATO: an object-oriented decision model to help on
563 irrigation scheduling for corn crop. *Ecological Modelling*, 137, 43-60.
- 564 Brisson, N., Mary, B., Ripoche, D., Jeuffroy, M.H., Ruget, F., Nicoullaud, B., Gate, P.,
565 Devienne-Barret, F., Antonioletti, R., Durr, C., Richard, G., Beaudoin, N., Recous, S.,

- 566 Tayot, X., Plenet, D., Cellier, P., Machet, J.-M., Meynard, J.M. & Delécolle, R. 1998
567 STICS: a generic model for the simulation of crops and their water and nitrogen
568 balances. I. Theory and parametrization applied to wheat and corn. *Agronomie*, 18,
569 311–346.
- 570 Chevalier, C., Picheny, V., & Ginsbourger, D. 2014. KrigInv: An efficient and user-
571 friendly implementation of batch-sequential inversion strategies based on kriging.
572 *Computational Statistics & Data Analysis*, 71, 1021-1034,
573 [dx.doi.org/10.1016/j.csda.2013.03.008](https://doi.org/10.1016/j.csda.2013.03.008).
- 574 Constantin, J., Willaume, M., Murgue, C., Lacroix, B. & Therond, O. 2015. The soil-
575 crop models STICS and AqYield predict yield and soil water content for irrigated crops
576 equally well with limited data. *Agricultural and Forest Meteorology*, 206, 55-68. doi:
577 [10.1016/j.agrformet.2015.02.011](https://doi.org/10.1016/j.agrformet.2015.02.011)
- 578 Cressie, N.A.C. 2015. *Statistics for Spatial Data*. Wiley-Interscience. 899 p.
- 579 Czyz, E. & Dexter, A.R. 2012. Plant wilting can be caused either by the plant or by the
580 soil. *Soil Research*, 50, 708-713. [dx.doi.org/10.1071/SR12189](https://doi.org/10.1071/SR12189)
- 581 Guérif, M., Houlès, V., Makowski, D. & Lauvernet, C. 2006. Data assimilation and
582 parameter estimation for precision agriculture using the crop model STICS. In: Wallach
583 D., Makowski D., Jones J.W., (Eds.), *Working with Dynamic Crop Models*. Elsevier.
- 584 Keating, B.A., Carberry, P.S., Hammer, G.L., Probert, M.E., Robertson, M.J.,
585 Holzworth, D., Huth, N.I., Hargreaves, J.N.G., Meinke, H., Hochman, Z., McLean, G.,
586 Verburg, K., Snow, V., Dimes, J.P., Silburn, M., Wang, E., Brown, S., Bristow, K.L.,
587 Asseng, S., Chapman, S., McCown, R.L., Freebairn, D.M. & Smith, C.J. 2003. An

- 588 overview of APSIM, a model designed for farming systems simulation. *European*
589 *Journal of Agronomy*, 18, 267–288.
- 590 Lawless, C., Semenov, M.A. & Jamieson, P.D. 2008. Quantifying the effect of
591 uncertainty in soil moisture characteristics on plant growth using a crop simulation
592 model. *Field Crops Research* 106, 138–147.
- 593 Ma, L., Ahuja, L.R., Islam, A., Trout, T.J., Saseendrand, S.A. & Malone, R.W. 2017.
594 Modeling yield and biomass responses of maize cultivars to climate change under full
595 and deficit irrigation. *Agricultural Water Management*, 180, 88–98. doi:
596 10.1016/j.agwat.2016.11.007
- 597 Nendel, C., Kersebaum, K.C., Mirschel W. & Wenkel, K.O. 2014. Testing farm
598 management options as climate change adaptation strategies using the MONICA model.
599 *European Journal of Agronomy*, 52, 47–56. doi: 10.1016/j.eja.2012.09.005
- 600 Palosuo, T., Kersebaum, K.C., Angulo, C., Hlavinka, P., Moriondo, M., Olesen, J.E.,
601 Patil, R.H., Ruget, F., Rumbaur, C., Takáč, J., Trnka, M., Bindi, M., Çaldağ, B., Ewert,
602 F., Ferrise, R., Mirschel, W., Şaylan, L., Šiška, B. & Rötter, R.P. 2011. Simulation of
603 winter wheat yield and its variability in different climates of Europe: A comparison of
604 eight crop growth models. *Eur. J. Agron.* 35, 103–114. doi:10.1016/j.eja.2011.05.001
- 605 Pandey, R.K., Maranville, J.W. & Chetima, M.M. 2000. Deficit irrigation and nitrogen
606 effects on maize in a Sahelian environment II. 2-Shoot growth, nitrogen uptake and
607 water extraction. *Agricultural Water Management*, 46, 15–27.
- 608 Picheny, V., Ginsbourger, D., Roustant, O., Haftka, R.T. & Kim, N-H. 2010. Adaptive
609 designs of experiments for accurate approximation of a target region. *Journal of*
610 *Mechanical Design*, 132, 071008. doi:10.1115/1.4001873

- 611 Qian, P.Z.G., Huaiqing, W. & Wu, C.F.J. 2008. Gaussian process models for computer
612 experiments with qualitative and quantitative factors. *Technometrics*, 50, 383-396.
- 613 R Core Team, 2014. R: A language and environment for statistical computing. R
614 Foundation for Statistical Computing, Vienna, Austria.
- 615 Ritchie, J.T. 1981. Water dynamics in the soil-plant-atmosphere system. *Plant Soil*, 58,
616 81–96. doi:10.1007/BF02180050
- 617 Ranatunga, K., Nation, E.R. & Barratt D.G. 2008. Review of soil water models and
618 their applications in Australia, *Environmental Modelling & Software*, 23, 1182–1206.
619 dx.doi.org/10.1016/j.envsoft.2008.02.003
- 620 Rötter, R.P., Palosuo, T., Kersebaum, K.C., Angulo, C., Bindi, M., Ewert, F., Ferrise,
621 R., Hlavinka, P., Moriondo, M., Nendel, C., Olesen, J.E., Patil, R.H., Ruget, F., Takáč,
622 J. & Trnka, M. 2012. Simulation of spring barley yield in different climatic zones of
623 Northern and Central Europe: A comparison of nine crop models. *F. Crop. Res.* 133,
624 23–36. doi:10.1016/j.fcr.2012.03.016
- 625 Roustant, O., Ginsbourger, D. & Deville, Y. 2012. “DiceKriging, DiceOptim: Two R
626 Packages for the Analysis of Computer Experiments by Kriging-Based Metamodeling
627 and Optimization.” *Journal of Statistical Software*, 51(1), 1–55.
- 628 Spiegelhalter, D.J. & Riesch, H. 2011. Don’t know, can’t know: embracing deeper
629 uncertainties when analysing risks. *Phil. Trans. R. Soc. A* 369, 4730–4750.
630 doi:10.1098/rsta.2011.0163

- 631 Teegavarapu, R.S.V. 2010. Modeling climate change uncertainties in water resources
632 management models. *Environmental Modelling & Software*, 25,1261–1265. doi:
633 10.1016/j.envsoft.2010.03.025
- 634 Vanuytrecht, E., Raes, D. & Willems, P. 2014. Global sensitivity analysis of yield
635 output from the water productivity model. *Environmental Modelling & Software* 51,
636 323-332.
- 637 Varella, H., Buis, S., Launay, M. & Guérif, M. 2012. Global sensitivity analysis for
638 choosing the main soil parameters of a crop model to be determined. *Agri. Science* 3,
639 949–961.
- 640 Veihmeyer, F.J. & Hendrickson, A.H. 1949. Methods of measuring field capacity and
641 permanent wilting point. *Soil Science* 68 (1), 75-94.
- 642 Walker, W.E., Harremoes, P., Rotmans, J., Van der Sluijs, J.P., van Asselt, M.B.A.,
643 Janssen, P. & Kraymer von Krauss, M.P. 2003. A Conceptual Basis for Uncertainty
644 Management in Model-Based Decision Support. *Integr. Assess.* 0, 1–13.
- 645 Wösten, J.H.M., Lilly, A., Nemes, A. & Le Bas, C. 1999. Development and use of a
646 database of hydraulic properties of European soils. *Geoderma* 90, 169-185.
- 647 Zhang, H. & Oweis, T. 1999. Water-yield relations and optimal irrigation scheduling of
648 wheat in the Mediterranean region. *Agricultural Water Management*, 38, 195–211.

649 **TABLES**

650 **Table 1.** Factors simulated and outputs analyzed in the simulation experiment. Each
 651 crop was simulated in all soils and sites. A given climate type differs according to the
 652 site (i.e. the Hot&Dry climate is hotter and drier in Toulouse than it is in Poitiers).

Crops	Species	Sunflower	Winter wheat
	Sowing & harvest dates	1 May - 1 Oct	1 Oct - 10 Jul
	Flowering & maturity	1120-1720°C-days	1300-2015°C-days
Soils	Depth	Shallow - 0.8 m, Deep - 1.5 m	
	Available water capacity	Shallow - 80-140 mm, Deep - 140-240 mm	
Climate	Site (coordinates)	Toulouse (43° 33'N, 1° 26'E), Poitiers (46° 33'N, 0° 17'E)	
	Climate types by site	Cold&Dry, Hot&Dry, Cold&Wet, Hot&Wet	
Outputs		Crop yield, Water drainage	

653

654

655 **Table 2.** Characteristics of the four years selected for each site during crop development.
 656 Thermal time (TT) is the sum of temperatures between sowing and harvest calculated
 657 with a base temperature of 0°C for wheat and 4.8°C for sunflower. WD_c is the water
 658 deficit, calculated as the difference between precipitation and potential evapotranspiration
 659 during the crop development period.

Characteristic	Climate	Sunflower		Winter wheat	
		Toulouse	Poitiers	Toulouse	Poitiers
TT (°C-days)	Cold&Wet	2010	1752	2669	2282
	Cold&Dry	2113	1823	2599	2348
	Hot&Wet	2281	1966	2897	2545
	Hot&Dry	2336	1999	3011	2643
WD_c (mm)	Cold&Wet	-238	-167	114	271
	Cold&Dry	-402	-321	-18	7
	Hot&Wet	-403	-227	-90	249
	Hot&Dry	-572	-388	-249	58

660

661

662 **Table 3.** Critical region at 5%, 10% or 15% thresholds of variation for each output
 663 according to uncertainty in available water capacity (AWC). Darker shading indicates
 664 higher values. On average, AWC ranged from 80-140 mm and 140-240 mm for shallow
 665 and deep soil, respectively. *NA: drainage under the crop is null regardless of the
 666 AWC.
 667

Climate	Site	α	Critical region graphs for yield				Critical region graphs for drainage			
			Sunflower		Winter wheat		Sunflower		Winter wheat	
			Shallow soil	Deep soil	Shallow soil	Deep soil	Shallow soil	Deep soil	Shallow soil	Deep soil
Hot&Dry	Toulouse	0.05	0.72	0.02	0.44	0.01	NA*	NA	0.31	0.00
		0.10	0.40	0.00	0.06	0.00			0.01	0.00
		0.15	0.06	0.00	0.00	0.00			0.00	
	Poitiers	0.05	0.95	0.20	0.36		0.99			
		0.10	0.88	0.09	0.01	0.00	0.97	NA	0.00	0.00
		0.15	0.81	0.03	0.00		0.96			
Cold&Dry	Toulouse	0.05	0.73	0.02	0.24		0.53	0.07	0.22	
		0.10	0.43	0.00	0.05	0.00	0.23	0.00	0.00	0.00
		0.15	0.16	0.00	0.00		0.08	0.00	0.00	
	Poitiers	0.05	0.83	0.08			0.71	0.39		
		0.10	0.63	0.00	0.00	0.00	0.42	0.03	0.00	0.00
		0.15	0.43	0.00			0.13	0.00		
Hot&Wet	Toulouse	0.05	0.68	0.02	0.10		0.42	0.01		
		0.10	0.34	0.00	0.00	0.00	0.01	0.00	0.00	0.00
		0.15	0.10	0.00	0.00		0.00	0.00		
	Poitiers	0.05	0.13		0.12		0.99	0.95		
		0.10	0.01	0.00	0.00	0.00	0.97	0.90	0.00	0.00
		0.15	0.00		0.00		0.95	0.84		
Cold&Wet	Toulouse	0.05	0.35				0.92	0.82		
		0.10	0.06	0.00	0.00	0.00	0.83	0.63	0.00	0.00
		0.15	0.00				0.75	0.45		
	Poitiers	0.05	0.52				0.20			
		0.10	0.21	0.00	0.00	0.00	0.00	0.00	0.00	0.00
		0.15	0.06				0.00			

668

669 FIGURE CAPTIONS

670 **Figure 1.** Conceptual diagram of the AqYield model. PET is potential evapotranspiration,
671 P+I is precipitation plus irrigation, T is temperature and AWC is available water capacity
672 for crops.

673 **Figure 2.** Sample illustration of the threshold graph. The x-axis shows mean available
674 water capacity (AWC), ranging from 80-140 mm for shallow soils and, not shown, 140-
675 240 mm for deep soils. The y-axis shows the standard deviation of AWC, ranging from
676 0-50 mm. A: areas in which the coefficient of variation (CV) exceeds all three thresholds
677 (5%, 10% and 15%); B: area in which the CV does not exceed either 5%, 10% or 15%
678 threshold; C: thresholds between A and B (depending on the threshold chosen). X^* :
679 average AWC above which the CV is always non-critical (for $\alpha < 15\%$), regardless of the
680 standard deviation (up to 50 mm), Y^* : standard deviation below which the CV is always
681 non-critical (for $\alpha < 15\%$), regardless of the average AWC.

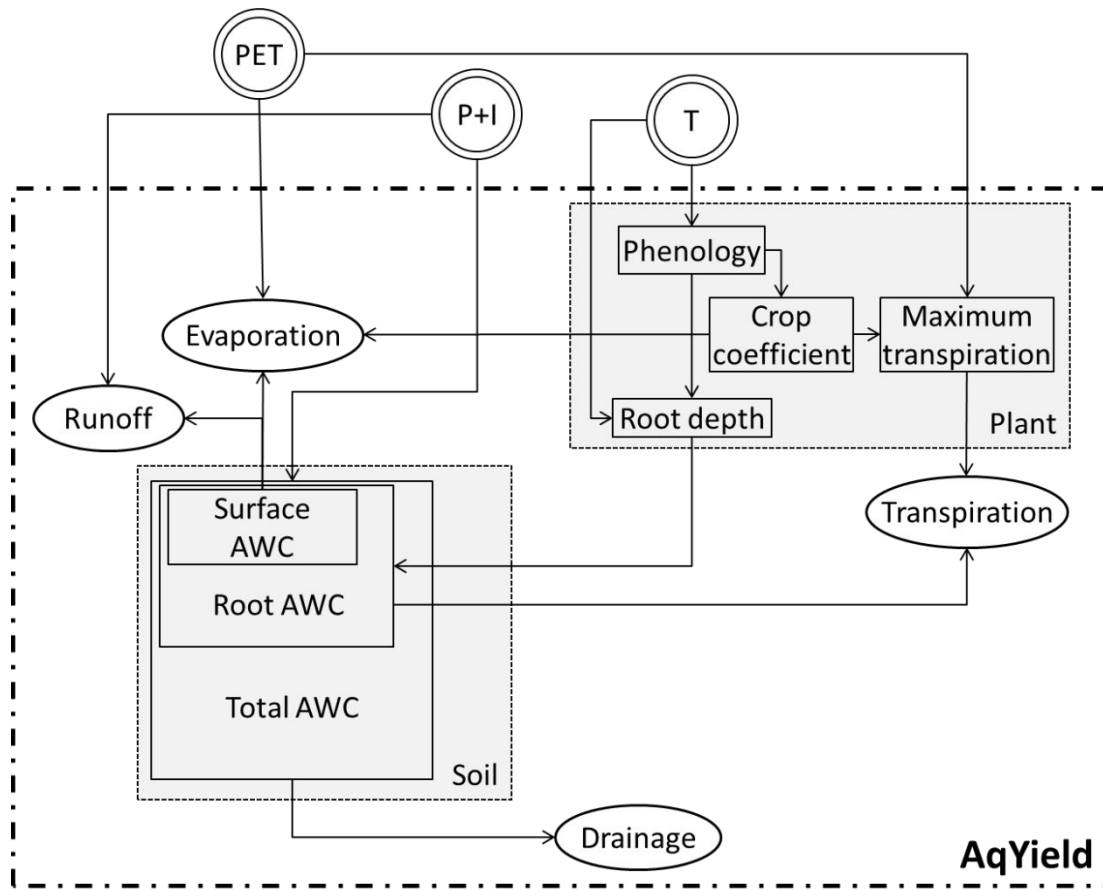
682 **Figure 3.** Representation of the climates (cumulative precipitation minus potential
683 evapotranspiration (P-PET) as a function of thermal time) of (a and c) Poitiers and (b and
684 d) Toulouse for 1975-2012 (circles) during the development periods of (a and b)
685 sunflower (1 May – 1 October) and (c and d) winter wheat (1 October – 10 July). Each
686 graph is divided into four types of climates: warm and wet (green), warm and dry (red),
687 cold and wet (blue) and cold and dry (purple). Triangles indicate means of all climate
688 years.

689 **Figure 4.** Predicted mean yield of (a) sunflower and (c) wheat and mean drainage under
690 (b) sunflower and (d) wheat according to crop, type of climate and soil depth when AWC
691 varies uniformly from 30-190 mm and 90-290 mm for shallow and deep soil, respectively.

692 Error bars represent the standard deviation due to the variation in AWC (30-190 and 90-
693 290 mm according to the soil type).

694 **Figure 5.** Threshold graphs for yield and drainage according to type of climate, site, soil
695 depth and crop (described in Fig. 2). The x-axis shows mean available water capacity
696 (AWC), ranging from 80-140 mm for shallow soil and 140-240 mm for deep soil. The y-
697 axis shows the standard deviation of AWC, ranging from 0-50 mm (as in Fig. 2). The
698 three thresholds of 5%, 10% and 15% are represented on the graphs if relevant (dark gray
699 <5%, gray > 5%, light gray > 10% and very light gray > 15%). NA: drainage under the
700 crop is null regardless of the AWC.

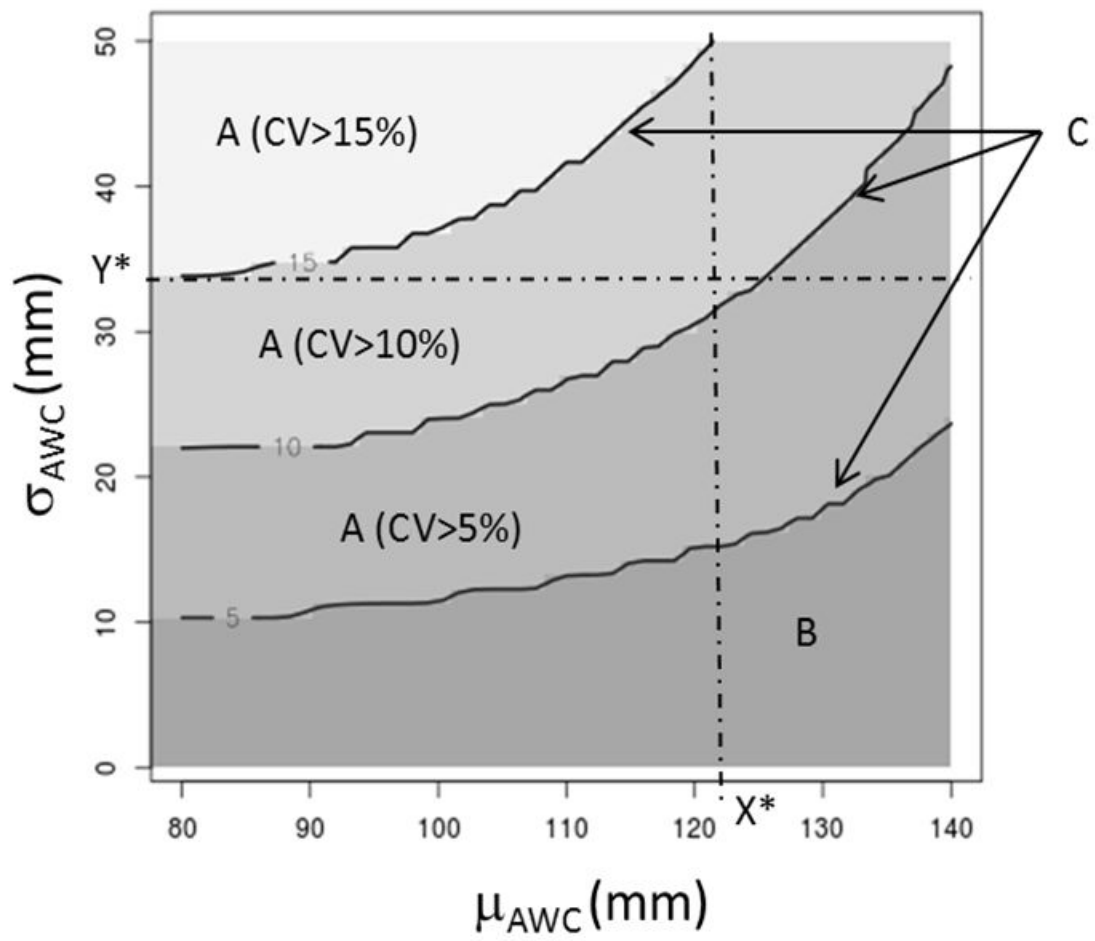
701



702

703 Figure 1

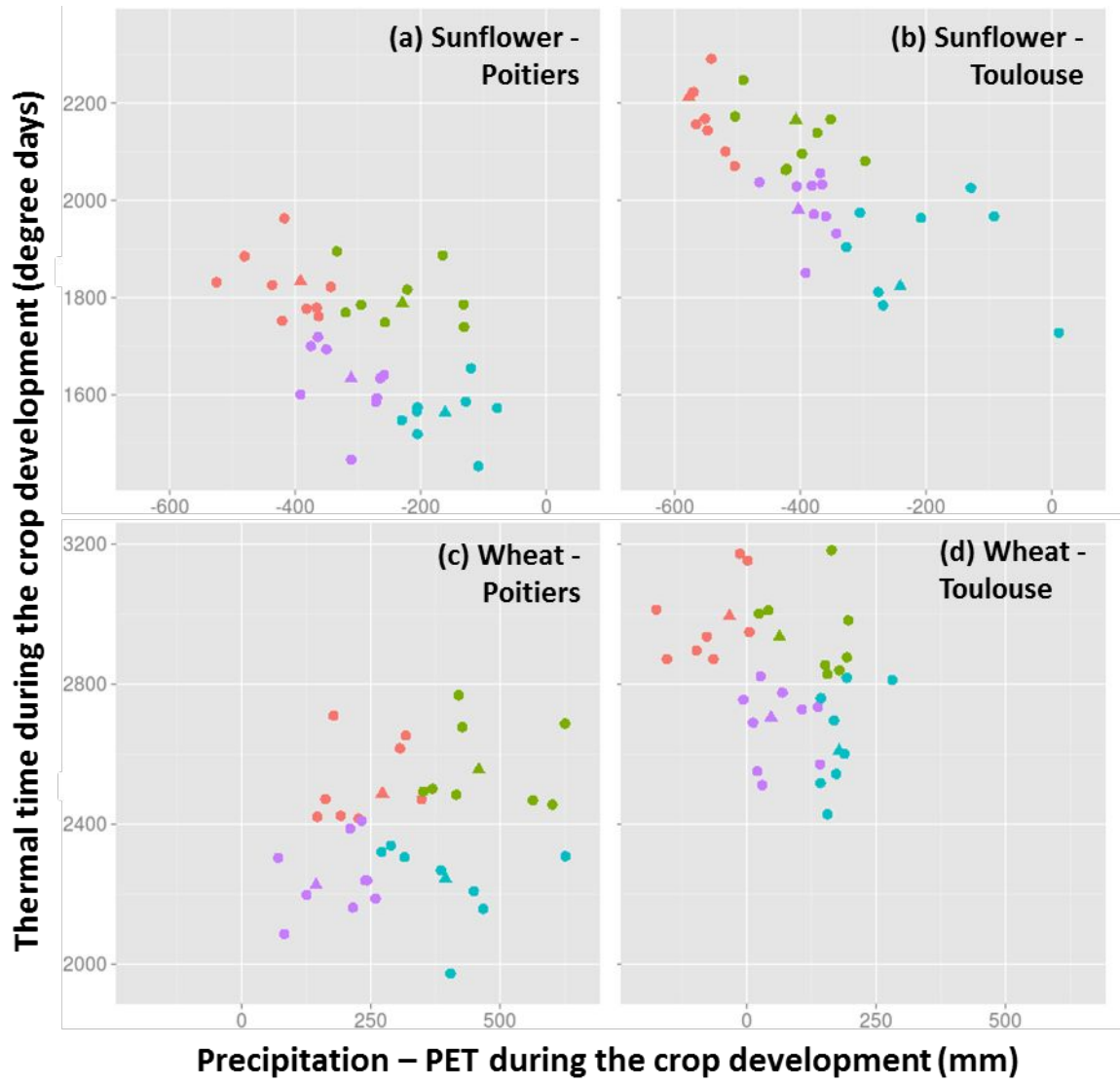
704



705

706 Figure 2

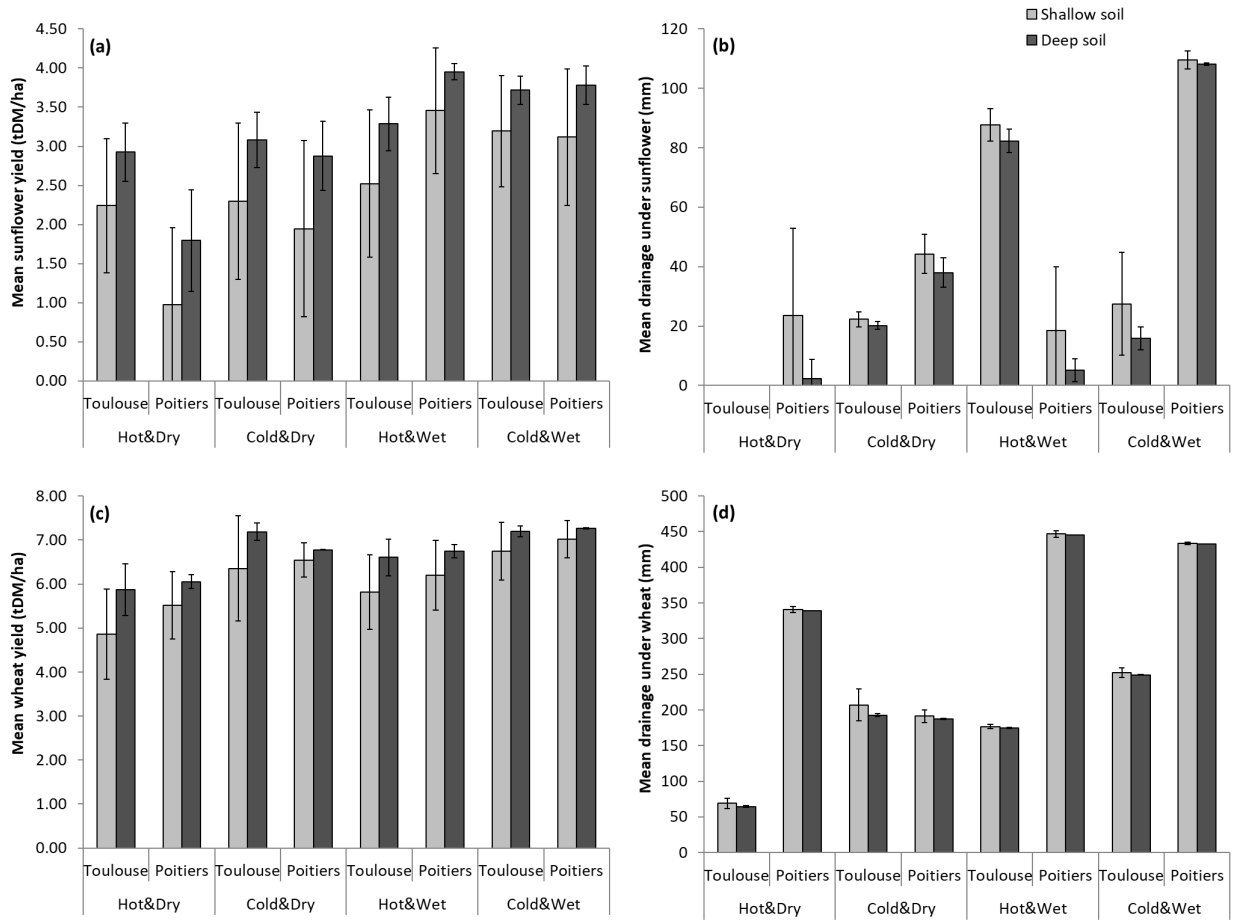
707



708

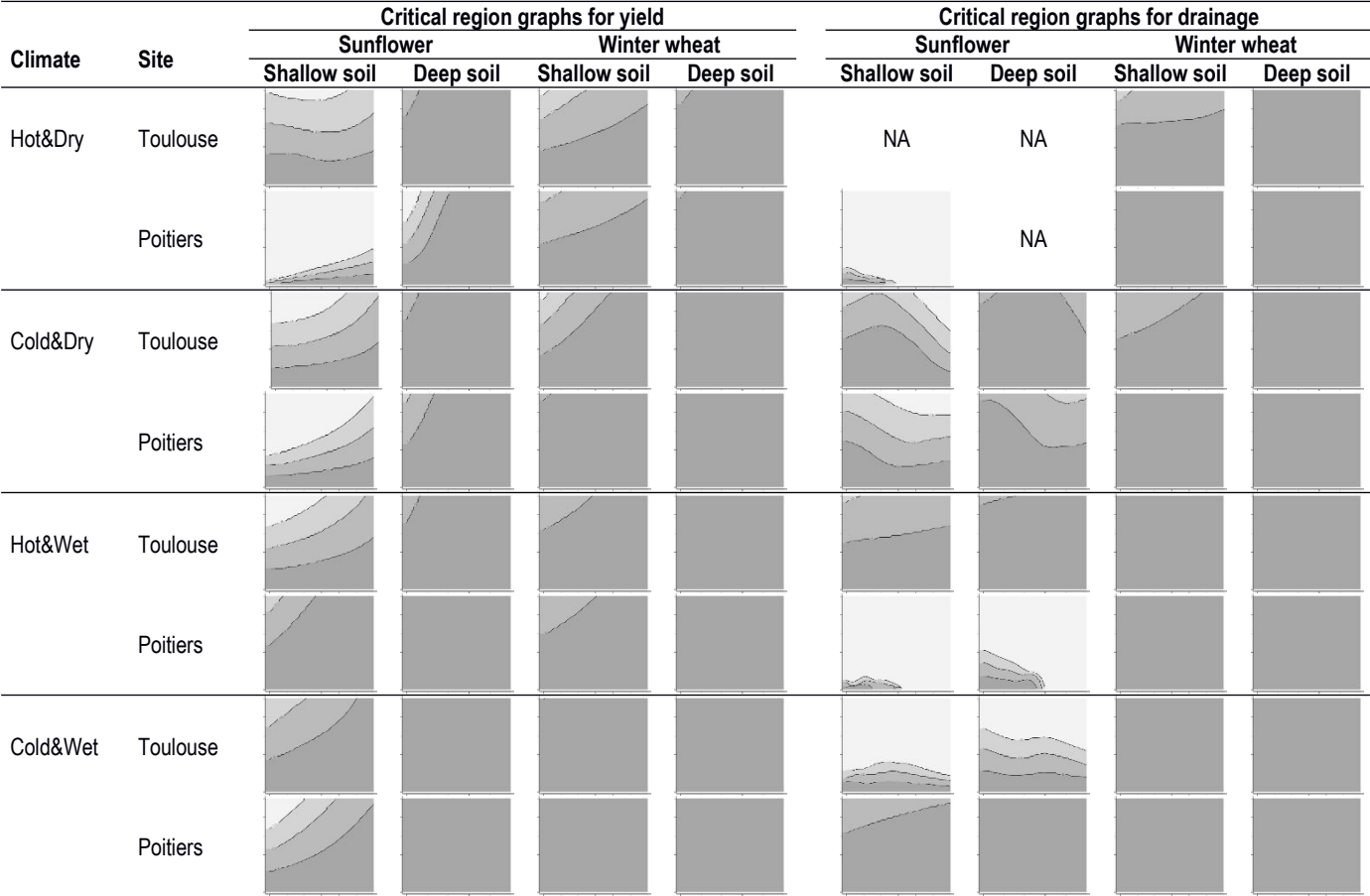
709 Figure 3

710



711

712 Figure 4



713 Figure 5

714 **Supporting Information**

715

716 In our simulation experiment, kriging models were fitted using the R package

717 DiceKriging (Roustant et al., 2012) with the default options, in particular a constant trend

718 (i.e. *ordinary kriging*) and Matérn covariance, as described below. Provided a set of n719 observations $(x_1, f_1), \dots, (x_n, f_n)$ and given a covariance function c , the kriging predictor720 for any \mathbf{x} is equal to:

721
$$m(\mathbf{x}) = \hat{m} + c_n(\mathbf{x})C_n^{-1}(F_n - \hat{m}\mathbf{1}_n)$$

722 with:

723 • $F_n = (f_1, \dots, f_n)^T$ the vector of observed values,724 • $C_n = (c(x_i, x_j))_{1 \leq i, j \leq n}$ a n x n covariance matrix,725 • $c_n(\mathbf{x}) = (c(x_1, \mathbf{x}), \dots, c(x_n, \mathbf{x}))^T$ a covariance vector,726 • $\mathbf{1}_n$ is a n x 1 vector of ones, and727 • $\hat{m} = \frac{\mathbf{1}_n^T C_n^{-1} F_n}{\mathbf{1}_n^T C_n^{-1} \mathbf{1}_n}$ is a constant.728 Here, \mathbf{x} corresponds to a pair (μ_X, σ_X) and f to the corresponding *CV*.729 In general, kriging models depend largely on the covariance function c , for which a large

730 catalogue is available in the literature. We used the default value of the DiceKriging

731 package, which is the Matérn kernel with shape parameter 3/2, defined as:

732
$$c(\mathbf{x}, \mathbf{x}') = \sigma^2 \left(1 + \sqrt{3} \sum_1^2 \frac{|x_i - x'_i|}{\theta_j} \right) \exp \left(- \sum_1^2 \frac{|x_i - x'_i|}{\theta_j} \right)$$

733 which depends on parameters $\sigma^2, \theta_1, \theta_2$, which are estimated by maximum likelihood

734 within DiceKriging.

735 One advantage of the kriging model is its probabilistic interpretation (Cressie, 2015),
 736 since it also provides a local error estimate, often referred to as *prediction variance*, equal
 737 to:

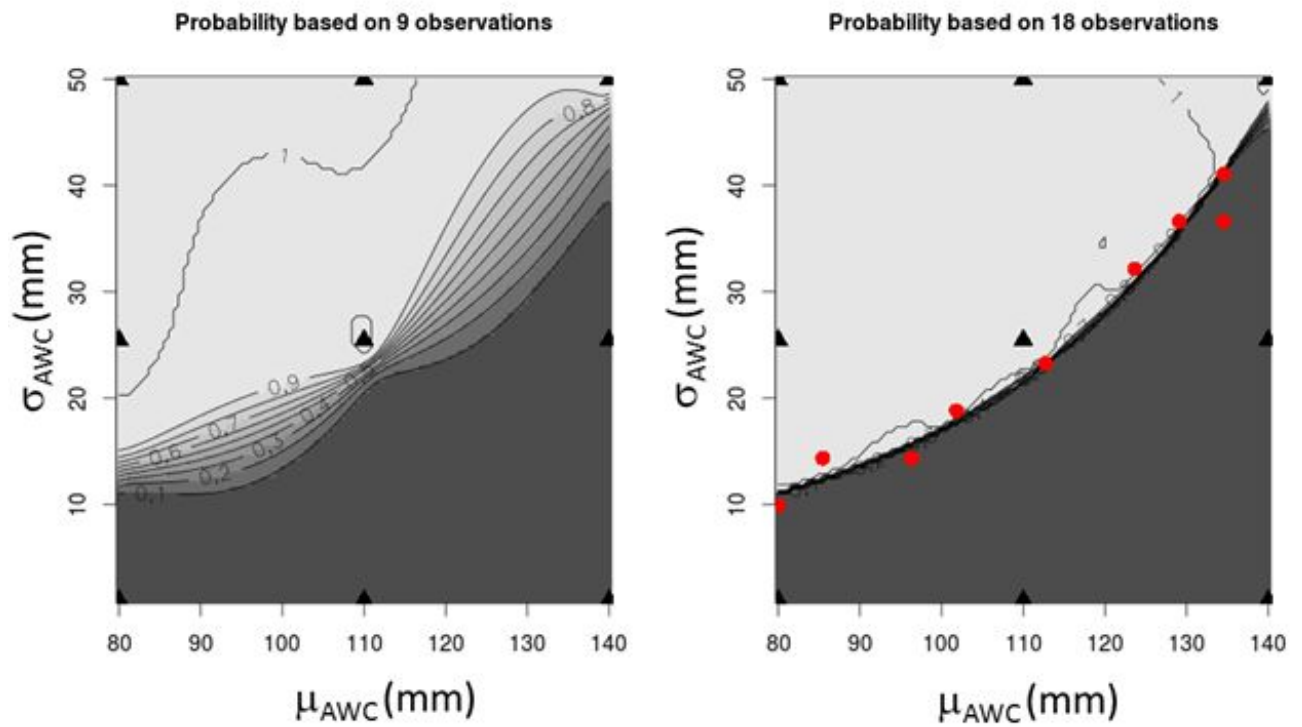
$$738 \quad s(x)^2 = \sigma^2 - c_n(x)^T C_n^{-1} c_n(x) + \frac{(1 - \mathbf{1}_n^T C_n^{-1} c_n(x))^2}{\mathbf{1}_n^T C_n^{-1} \mathbf{1}_n}$$

739 In our context, we used this information to compute the probability, given a set of
 740 observations $(x_1, f_1), \dots, (x_n, f_n)$, that the *CV* at a point x exceeds α . This probability is
 741 equal to

$$742 \quad P(x) = \Phi\left(\frac{\alpha - m(x)}{s(x)}\right)$$

743 with Φ the cumulative distribution function of the standard normal law. Probabilities
 744 close to 0.5 indicate that the kriging prediction is inaccurate (large s), while probabilities
 745 close to 0 or 1 show accurate prediction with respect to the classification objective (below
 746 or over the threshold, respectively).

747 In an illustration of the kriging strategy (Fig. S1), the soil, climate and crop are fixed,
 748 while the AWC mean and standard deviation vary between lower and upper bounds (μ_x
 749 = 80-140 mm and $\sigma_x = 0$ -50 mm). We consider the yield for Y and the threshold $\alpha = 10\%$.
 750 We represent the probability of exceeding α at the initial stage (based on 9 observations)
 751 and after the sequential procedure (based on 18 observations).



752

753 After the initial observation stage (Fig. A1, left), the critical set Ω_c is identified only
 754 roughly (large region with values close to 0.5), while after the sequential procedure
 755 (Fig. A1, right), the probability is either close to 0 or 1 everywhere, indicating that the
 756 critical region (Fig. A1, white) was accurately determined, due to the additional
 757 observations next to its boundary.